Molecular Phylogenetics and Evolution 127 (2018) 416–428

Contents lists available at ScienceDirect

Molecular Phylogenetics and Evolution

journal homepage: www.elsevier.com/locate/ympev

Transoceanic Stepping–stones between Cretaceous waterfalls? The enigmatic biogeography of pantropical *Oocyclus* cascade beetles

Emmanuel F.A. Toussaint[a,b,*], Andrew E.Z. Short[a]

[a] Department of Ecology & Evolutionary Biology & Division of Entomology, Biodiversity Institute, University of Kansas, Lawrence, KS 66045, USA
[b] Florida Museum of Natural History, University of Florida, Gainesville, FL 32611, USA

ARTICLE INFO

Keywords:
Comparative biogeography
Diversification
Gondwana
Hydrophilidae
Laurasia
Seepage habitats

ABSTRACT

Beetles have colonized freshwater habitats multiple times throughout their evolutionary history. Some of these aquatic lineages are associated exclusively with waterfall–like habitats, often with modified morphologies to cope with their unusual way of life. The historical biogeography of such cascade beetle lineages has been shown to strongly reflect ancient tectonic events. We focus on the pantropical genus *Oocyclus* of which species dwell in waterfalls and associated habitats. We infer the first molecular phylogeny of *Oocyclus* using a dataset of seven gene fragments. We recover a well resolved phylogenetic hypothesis, with a monophyletic *Oocyclus* divided in three genetically well–differentiated subclades which correspond to geography. Comparative dating analyses across Hydrophilidae based on ten fossil calibrations recover a Cretaceous origin for the genus. Based on a comprehensive suite of ancestral range analyses, we suggest a unique pattern with an origin in Southeast Asia followed by the successive colonization of India and the Neotropics via transoceanic stepping–stone dispersal. Diversification rate analyses support a scenario in which old *Oocyclus* lineages diversified slowly with a homogeneous rate regime. Waterfall beetle radiations are ancient and remarkably track Earth's paleogeological history, shedding light on intricate patterns of macroevolution.

1. Introduction

Deciphering the origin of biodiversity through geological time is a prime goal of evolutionary biology (Cox and Moore, 2010; Lomolino et al., 2010). At large geographic scales, biodiversity patterns between continents have fascinated biogeographers for centuries (e.g. Buffon, 1769; Von Humboldt, 1805; Darwin, 1859; Wallace, 1876). In the early stages of biogeography, dispersal was the dominant force proposed to explain disjunct distributions. Following the discovery of plate tectonics (Wegener, 1912), vicariance gained more attention, and soon became the exclusive scenario to explain the biogeographical history of clades that displayed disjunct geographic ranges. However, the advent of molecular phylogenies resulted in a further shift in paradigm, because a substantial fraction of accepted examples of vicariance could not be reconciled with divergence time estimates (de Queiroz, 2005). Since then, substantiated empirical examples of Pangean, Laurasian, or Gondwanan vicariance have become much more infrequent. Pangean vicariance whereby Laurasian and Gondwanan lineages would have split in the Jurassic and later diverged through allopatric speciation has therefore rarely been suggested (e.g. Mao et al., 2012; Murienne et al., 2014). Later vicariant events invoking the breakup of Gondwana as a favored scenario are less infrequent but remain uncommon. Examples of West Gondwanan vicariance invoking the split between Africa and South America have only been suggested by a few recent empirical studies using molecular dating (e.g. Gamble et al., 2008; Berger et al., 2016; Cai et al., 2016; Eberle et al., 2017; Luebert et al., 2017; Toussaint et al., 2017a). On the other side of the supercontinent, East Gondwanan vicariance has been suggested in several clades, between Australia and Madagascar (e.g. Thomas et al., 2014), Australia and South America (e.g. Kim and Farrell, 2015; Mennes et al., 2015; Milner et al., 2015; Toussaint et al., 2017b), or India/Seychelles and Madagascar (e.g. Toussaint et al., 2016). Several of these old vicariant scenarios have been suggested for water beetles, a non–monophyletic group which comprises lineages with remarkable disjunct distributions (e.g. Bilton et al., 2015; Toussaint et al., 2016, 2017a,b; Toussaint & Short, 2017), and has therefore been an emerging model for biogeographic studies.

Here we focus on the pantropical genus *Oocyclus* (Coleoptera, Hydrophilidae, Laccobiini). This genus is comprised of 66 described species as well as approximately 20 species awaiting description (Short et al., in prep.). These beetles are found in habitats associated with waterfalls and seepages in India/Sri Lanka, the Oriental region and the

* Corresponding author at: Florida Museum of Natural History, University of Florida, Gainesville, FL 32611, USA.
E-mail address: Emmanuel.touss1@gmail.com (E.F.A. Toussaint).

https://doi.org/10.1016/j.ympev.2018.04.023
Received 21 December 2017; Received in revised form 7 April 2018; Accepted 15 April 2018
Available online 07 May 2018
1055-7903/

Neotropics. They have never been found in the Afrotropics, Australasia, Nearctic or Palearctic and other parts of the supercontinent Gondwana (e.g. New Caledonia; New Zealand). Despite this intricate distribution pattern, there is no phylogenetic hypothesis for the genus to date. Few species were included in a large–scale phylogeny for the family Hydrophilidae where the genus was found paraphyletic (Short and Fikáček, 2013). Subsequent works based on this latter molecular dataset inferred an age for the crown of *Oocyclus* in the Cretaceous (Bloom et al., 2014; Toussaint et al., 2016).

We infer the most comprehensive phylogeny of the superfamily Hydrophiloidea using a new molecular dataset of the tribe Laccobiini, combined with multiple recently published others (Bernhard et al., 2006; Short and Fikáček, 2013; Toussaint et al., 2016; 2017a; Short et al., 2017a,b). Using a set of robust fossil calibrations we infer divergence time estimates for the superfamily and focus on the genus *Oocyclus*. We specifically aim to estimate the historical biogeography of the genus using a comparative framework, while weighing the impact of divergence time estimate uncertainty, outgroup inclusion, biogeographic model parameters, and potential diversification rate shifts.

2. Material and methods

2.1. Taxon sampling and molecular biology

We assembled the largest taxon and molecular sampling to date for the family Hydrophilidae using the datasets of Bernhard et al. (2006), Short & Fikáček (2013), Toussaint et al. (2016, 2017a), and Short et al. (2017a,b), along with 58 newly sequenced species from different genera of the tribe Laccobiini (i.e. *Laccobius*, *Oocyclus* and *Pelthydrus*). We added 43 species of the genus *Oocyclus* collected in different biogeographic regions (see Table S1). Based on our expertise and current taxonomy, the genus has an estimated species richness of about 87 species, 66 of which have already been described. There are six described species and one known undescribed species of *Oocyclus* in South India and Sri Lanka, 16 described in China and Southeast Asia with at least 4 known undescribed species, and 44 described species in the Neotropics, with at least 16 undescribed species (Short in prep.). In this study, we sampled 3 species from South India/Sri Lanka (~55% of the species when including *Ophthalmocyclus*, see Results), 11 from China/Southeast Asia (~57% of the species), and 37 from the Neotropics (~62% of the species), for a total of 51 *Oocyclus* species (when including *Ophthalmocyclus*, see Results), representing ~60% of the species richness. We included multiple outgroups from closely related families of Hydrophiloidea as well as *Spercheus emarginatus* (Spercheidae) to root the topology (Bernhard et al., 2006). A complete list of included taxa is provided in Table S1.

Total genomic DNA was extracted from whole beetles kept in 96% ethanol using the DNeasy kit (Qiagen, Hilden, Germany). All vouchers are deposited at the University of Kansas (Lawrence, USA). We used the PCR protocols of Short and Fikáček (2013) and Baca et al. (2017) to amplify and sequence seven gene fragments, the six comprised in Short and Fikáček (2013); ribosomal 16S (16S, 787 bp), ribosomal 18S (18S, 1852 bp), ribosomal 28S (1125 bp), arginine kinase (ARK, 705 bp), cytochrome oxidase subunit 1 (CO1, 768 bp), cytochrome oxidase 2 (CO2, 657 bp), and a fragment of histone 3 (H3, 327 bp). The DNA sequences were assembled and the contigs edited in Geneious R 8.1.9 (Biomatters, http://www.geneious.com/). We produced gene fragment alignments using MUSCLE (Edgar, 2004) for the protein–coding gene fragments (PCF), and MAFFT (Katoh & Standley, 2013) for the ribosomal gene fragments (RF) with manual adjusting in hypervariable regions. The reading frames of PCF were then checked in Mesquite 3.10 (build 765) (http://mesquiteproject.org). Details regarding gene fragment alignment compositions are given in Table S2. New sequences were deposited in GenBank (accession Nos MH317765–MH318010).

2.2. Molecular phylogenetics

Gene fragment topologies were inferred in a maximum likelihood (ML) framework using W–IQ–TREE 1.5 (Nguyen et al., 2015; Trifinopoulos et al., 2016). The gene fragment alignments were not partitioned and optimal models of substitution were selected in PartitionFinder 2 (Lanfear et al., 2017) among all available models using the greedy algorithm. The Bayesian Information Criterion (BIC) was used to compare the fit of the different models of substitution. To assess nodal support, we performed 2000 ultrafast bootstrap replicates (UFBS, Minh et al., 2013). Since the gene fragments did not show strongly supported inconsistencies, a full matrix was generated in Geneious R 8.1.9 by concatenating all gene fragment alignments.

We inferred phylogenetic relationships among Hydrophiloidea with Bayesian Inference (BI) using the full matrix alignment. The partitions and corresponding optimal models of substitution were selected in PartitionFinder 2, among the 'mrbayes' set of models, using the greedy algorithm and the BIC. The protein–coding gene fragments (PCF) were divided by codon position and the ribosomal gene fragments (RF) were left as unique partitions, for a total of 15 partitions. The BI analyses were performed using MrBayes 3.2.6 (Ronquist et al., 2012) as implemented on the CIPRES Science Gateway 3.3 (Miller et al., 2010). Two simultaneous and independent Metropolis–coupled Markov chain Monte Carlo analyses with eight chains (one cold and seven incrementally heated) running 100 million generations were used, with a tree sampling every 5000 generations to calculate posterior probabilities (PP). The convergence of the runs was assessed by investigating the average standard deviation of split frequencies in MrBayes and the Effective Sample Size (ESS) of all parameters in Tracer 1.6 (http://BEAST.bio.ed.ac.uk/Tracer). A value of ESS > 200 was used as a good indicator of convergence. All posterior trees that predated the time needed to reach a log–likelihood plateau were discarded as burn–in, and the remaining samples were summarized to generate a 50% majority rule consensus tree.

We also inferred a phylogenetic tree of Hydrophiloidea using W–IQ–TREE 1.5. The best partitioning scheme and models of substitutions were selected in PartitionFinder 2, among all available models, using the greedy algorithm and the BIC. To assess nodal support, we performed 2000 ultrafast bootstrap replicates.

Finally, we performed topological tests to assess the robustness of the placement of *Oocyclus* within Hydrophilidae (see Results and Fig. 1). We constrained *Oocyclus* (including *Ophthalmocyclus*, see Results) to be paraphyletic with the Southeast Asian clade being sister to *Arabhydrus*, *Hydrophilomima*, and *Pelthydrus* (see Results and Fig. 1), and compared the likelihood of the resulting topology with the non-constrained topology estimated in IQ-TREE (see above). We performed a Kishino-Hasegawa (KH) test (1989), Shimodaira-Hasegawa (SH) test (1999), expected likelihood weight (ELW) test (Strimmer & Rambaut, 2002), and an approximately unbiased (AU) test (Shimodaira, 2002) with 1000 RELL replicates (Kishino et al., 1990).

2.3. Divergence time estimation

Because preliminary analyses without topological constraint failed to converge (most ESS values of parameters < 100), we inferred divergence times using BEAST 1.8.3 (Drummond et al., 2012), with the fixed MrBayes topology. Since the different gene fragment alignments did not have identical taxon sampling (Table S2), we could not perform clock partitioning tests as implemented in ClockstaR (Duchêne et al., 2013). Instead, we conducted a series of partitioned analyses to find the best clock partitioning scheme among the ones tested. First (P1), we assumed a first partition for the mitochondrial gene fragments (MF), and a second partition for the nuclear gene fragments (NF). Second (P2), we assumed a first partition for the RF, a second partition for the nuclear PCF, and a third partition for the mitochondrial PCF. Third (P3), we unlinked all clock models except the MF. The models of

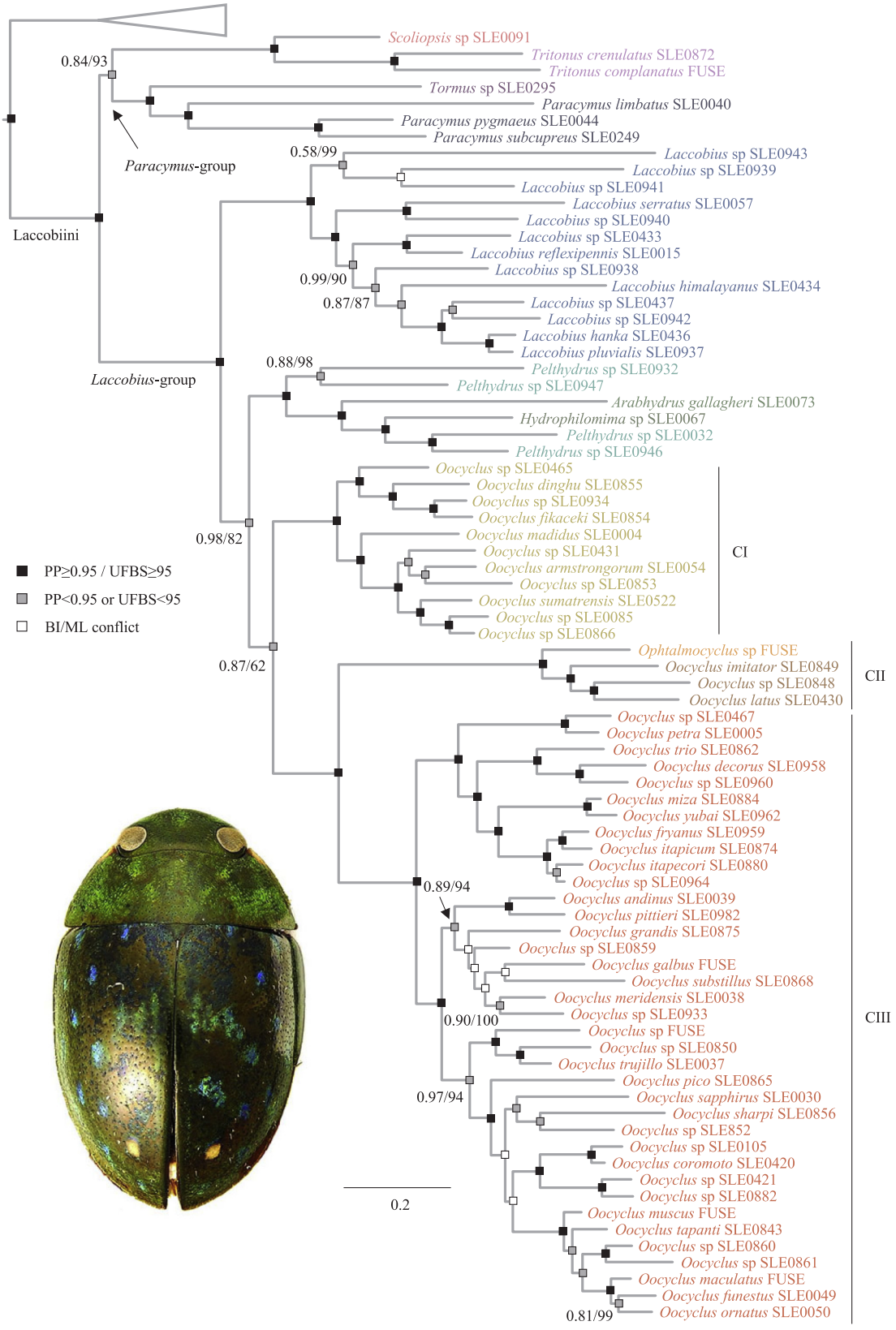

Fig. 1. Molecular phylogeny of the tribe Laccobiini Bayesian phylogenetic hypothesis inferred in MrBayes using the concatenated molecular matrix. Only the clade corresponding to Laccobiini is presented (see Figs. S1 and S2 for the full phylogeny). Nodal support values form the MrBayes (posterior probabilities, PP) and IQ-TREE (ultrafast bootstraps, UFBS) analyses are given according to the inserted caption. Different genera within Laccobiini are color-coded (the three major clades CI, CII and CIII within *Oocyclus* as well). A dorsal picture of *Oocyclus sapphirus* from Coastal Mountains in Venezuela is presented.

nucleotide substitution for each partition were selected under PartitionFinder 2, among the 'beast' set of models, using the 'greedy' algorithm and the BIC. The molecular clock test was performed in MEGA 7 (Kumar et al., 2016), by comparing the ML value of the MrBayes topology with and without the molecular clock constraints under the Tamura–Nei model. The null hypothesis of equal evolutionary rate throughout the tree was rejected at a 5% significance level (p-value < 0.001). Therefore, we used a Bayesian relaxed clock approach as implemented in BEAST 1.8.3. We assigned a lognormal relaxed clock with uncorrelated rates to each clock model. The Tree Model was set to Speciation: birth–death process. We used 10 fossils to calibrate the MrBayes phylogeny (Table S3): (1) *Baissalarva hydrobioides*† from the Baissa deposits in the Buryat Republic (Fikáček et al., 2014), dated back to the early Cretaceous (ca. 135 Ma, Zherikhin et al., 1998), was used to constrain the stem of Hydrobiusini; (2) *Cercyon* sp.† from Baltic amber (ca. 44 Ma, Kosmowska-Ceranowicz & Müller, 1985; Kosmowska-Ceranowicz, 1987; Ritzkowski, 1997), placed in the extant genus *Cercyon* by Kubisz (2000), but unambiguously assigned to Megasternini by Fikáček (pers. comm.), based on morphological features of the antennae and thorax, was used to constrain the stem of Megasternini; (3) *Crenitulus paleodominicus*† from Dominican amber (Fikáček & Engel, 2011), dated back to ca. 15–20 Ma (Iturralde-Vinent and MacPhee, 1996), was used to constrain the stem of *Crenitulus*, (4) *Helochares* sp.† from Baltic amber (Bloom et al., 2014), was used to constrain the stem of *Helochares*; (5) *Helophorus paleosibiricus*† from the Baissa deposits (Fikáček et al., 2012a,b), was used to constrain the stem of *Helophorus*; (6) *Hydrobiomorpha eopalpalis*† from the Messel pit in Germany (Fikáček et al., 2010a), dated from the mid–Eocene (ca. 47 Ma, Mertz & Renne, 2005), was used to constrain the stem of *Hydrobiomorpha*; (7) *Hydrobius titan*† described from the Florissant Formation in Colorado (ca. 34 Ma, Evanoff et al., 2001; Prothero & Sanchez, 2004), belongs to the extant genus *Sperchopsis* (Bloom et al., 2014), and was used to constrain the stem of this genus; (8) *Hydrochara* sp.† from the Messel pit (Fikáček et al., 2010a), was used to constrain the stem of *Hydrochara* (including the genus *Brownephilus* whose synonymy with *Hydrochara* is in preparation; Short et al., 2017b; Toussaint et al., 2017a); (9) *Limnoxenus olenus*† from Aix–en–Provence Formation (Fikáček et al., 2010b), dated back to ca. 22.5 Ma (Nury & Thomassin, 1994; Fikáček et al., 2010b), was used to constrain the stem of *Limnoxenus*; (10) *Protochares brevipalpis*† from the Talbragar Fossil Fish Bed (Fikáček et al., 2014), dated to the Late Jurassic (Turner et al., 2009; Beattie & Avery, 2012), was used to constrain the stem of Hydrophilidae.

We conservatively chose to use fossil calibrations as stem constraints following fossil morphological evidence (e.g., Fikáček et al., 2010a,b, 2014). Using crown constraint would have been perilous considering the lack of evidence that these fossils belong to the taxonomically-restricted clades sampled in this study. We used the minimum age of the stratum in which fossils were embedded to constrain focal nodes. The minimum ages were enforced with exponential and uniform distributions in different analyses to assess the impact of fossil calibration prior distributions on posterior divergence time estimates. The choice of a maximum age in dating analyses is always challenging, therefore we run two different kinds of analyses based on external estimates for the age of the superfamily Hydrophiloidea. There have been several attempts to calibrate the beetle tree of life in the past (Hunt et al., 2007; McKenna et al., 2015; Toussaint et al., 2017c). The most recent study conducted by Toussaint et al. (2017c) is a reanalysis of McKenna et al. (2015) based on a more extensive selection of 34 beetle fossil taxa. The resulting chronogram recovers a maximum age of about 215 million years (Myr) for the crown of Hydrophiloidea, and of about 273 Myr for its stem. Based on the reduced taxon sampling in Toussaint et al. (2017c), it is difficult to determine whether the crown or stem age should be used. Therefore, we used these two age estimates to enforce the uniform and exponential prior distributions for each fossil. Moreover, the root of the tree was calibrated with a uniform prior comprising as an upper bound the selected maximum age (215 or 273 Myr) and as a lower bound the minimum age of the oldest fossil used to calibrate the tree (i.e., 135 Myr). The exponential prior distribution parameters for each fossil calibration are given in Table S3. The parameter values were chosen so that the prior distribution would span the same interval as the one used in the uniform distributions, but with a diminishing tail of probability toward older ages (see Ho & Phillips, 2009 for a rationale).

The runs consisted of 200 million generations sampled every 5000 generations. We performed a marginal likelihood estimation using stepping–stone sampling (MLSS, Xie et al., 2011; Baele et al., 2012) for each run, using 1000 path steps, and chains running for one million generation with a log likelihood sampling every 1000 cycles. The MLSS were then calculated using BEAST. The convergence of the runs was investigated using ESS. A burn–in of 25% was applied after checking the log–likelihood curves. The maximum credibility trees, median ages and their 95% highest posterior density (HPD) were generated under TreeAnnotator 1.8.3 (Drummond et al., 2012).

2.4. Ancestral range estimation

The ancestral range estimations were performed on the chronogram resulting from the BEAST analysis with the best marginal likelihood (see Table S7 and Results). The chronogram was pruned to keep only the genus *Oocyclus* (including *Ophthalmocyclus*, see Results), hereafter referred to as *sensu stricto* (SS), or *Oocyclus* + *Ophthalmocyclus* as well as its sister clade comprising the genera *Arabhydrus*, *Hydrophilomima* and *Pelthydrus*, hereafter referred to as *sensu lato* (SL). These three latter genera are restricted to the Oriental region except for *Arabhydrus* whose distribution encompasses the Arabian Peninsula (one species). We used BioGeoBEARS (Matzke, 2013) to infer the biogeographical history of the genus across its entire range of distribution using both chronograms (SS and SL). This program allows the comparison of different models in a statistical framework. We ran and compared different analyses under the Dispersal Extinction and Cladogenesis (DEC, Ree et al., 2005; Ree and Smith, 2008), DIVA (Ronquist, 1997), and BAYAREA (Landis et al., 2013) models. The DIVA and BAYAREA models are implemented in a ML framework in BioGeoBEARS and as a result are respectively named DIVALIKE and BAYAREALIKE. We also ran the analyses with or without the founder–event jump dispersal parameter j (Matzke, 2014).

We used the following regions in the analyses: A, Andes; B, Brazilian Shield; C, Central America; G, Guiana Shield; I, India/Sri Lanka; and S, Oriental region. A seventh region corresponding to the Arabian Peninsula (P) was added in the analyses based on the SL chronogram. We designed three time slices to capture the main paleogeographical events that occurred during the evolution of the genus (Seton et al., 2012). The first time slice TS1 encompasses the period from the origin of the group about 110 million years ago (Ma) (120 Ma in SL, see Results) until 90 Ma when India separated from the rest of Gondwana. The second time slice TS2 stretches from 90 Ma to 55 Ma when India collided with the Eurasian plate. Finally, the last time slice TS3 covers the period between 55 Ma and the present. The dispersal rate scalers and adjacency matrices of the different time slices (Tables S4, S5 and S6) were chosen based on paleogeographic evidence following Seton et al. (2012). In all dispersal rate scaler matrices, dispersal events between adjacent areas were not scaled (dispersal $d = 1.0$). A scaler of 0.5 was applied for dispersal events between areas separated by a third one, and a scaler of 0.25 to dispersal events between areas separated by a small water barrier. Dispersal events between areas separated by a large oceanic barrier were considered long–distance dispersal events and were downweighted by a scaler of 0.1. We constrained the maximum number of ancestral areas to three. We also included a second model M2 penalizing over-water dispersal more and over-land dispersal less than in M1, namely with a dispersal rate scaler of 0.1 for any dispersal event over-water, and a dispersal scaler of 0.75 for dispersal events between areas separated by a third one. The analyses were also performed under a null model with all combinations of areas allowed and

no dispersal rate scalers (all d = 1.0).

2.5. Diversification analyses

We used the program R with the SL and SS chronograms to investigate diversification in a temporal framework while accounting for missing taxa in our sampling. To do so, we used the package TreePar (Stadler, 2011) to estimate the potential shifts in speciation and extinction rates in the two different chronograms via the function 'bd.shifts.optim'. This function uses the empirical branching times from the chronogram as an input and fits several birth–death models including 0 (constant–rate model) to several diversification rate shifts during the lineage evolution. We tested different models ranging from 0 to 3 rate shifts. All the analyses were carried out with the following non–default settings: taxon sampling was set to 52/87 (58/160 with SL), start = 0, end = 110 (120 with SL) and grid = 1 Myr for a fine–scale estimation of rate shifts. We calculated AICc scores and computed Likelihood Ratio Tests (LRT) to select the best–fit between the different models allowing incrementally more shifts during the evolution of the clade.

We also used the program Bayesian analysis of macroevolutionary mixture (BAMM 2.5, Rabosky, 2014; Rabosky et al., 2014), to estimate the macroevolutionary dynamics among and within the SL and SS chronograms. This program has recently been the object of criticism (Moore et al., 2016), and considering the ongoing debate regarding the accuracy of BAMM estimates (Rabosky et al., 2017), we remain cautious on the interpretation of the results in this study. Parameter priors were estimated using the command setBAMMpriors included in the R package BAMMtools (Rabosky et al., 2014). We conducted the BAMM analyses with four reversible jump MCMC (Huelsenbeck et al., 2004), running for 10 million generations and sampled every 5000 generations. We used a prior value for the compound Poisson process of 1.0 corresponding to a constant rate across the phylogeny. We considered non-random missing taxon sampling by assigning sampling ratios to the different clades recovered in the phylogeny based on our knowledge of the group and morphological affinities of missing taxa. ESS values were calculated using the R package CODA (Plummer et al., 2006). The output files were analyzed using BAMMtools. The posterior distributions of the BAMM analyses were used to estimate the best shift configurations and the 95% credible sets of distinct diversification models.

3. Results

3.1. Phylogenetic relationships

The topology resulting from the MrBayes analysis along with nodal support values of both analyses (BI and ML) is given in Fig. 1 for the tribe Laccobiini, and in Fig. 2 for the whole family Hydrophilidae (see Figs. S1 and S2 for detailed BI and ML trees). Both methods recovered highly similar phylogenetic relationships. We find the family Hydrophilidae monophyletic with strong support, as well as all subfamilies and tribes with moderate to strong support. Within the monophyletic tribe Laccobiini, we infer a clade comprised of *Paracymus*, *Scoliopsis*, *Tormus* and *Tritonus* as sister to all other genera. *Laccobius* is found monophyletic and as sister to a monophyletic clade comprised of *Oocyclus* and *Ophthalmocyclus* on one hand, and *Arabhydrus*, *Hydrophilomima*, and *Pelthydrus* on the other hand. The topological tests (KH, SH, ELW and AU) conducted in IQ-TREE did not significantly support the monophyly or the paraphyly of *Oocyclus*, with both tested topologies being statistically impossible to reject in all tests based on our dataset (Table 1). However, the clade comprised of *Oocyclus* and *Ophthalmocyclus* is found monophyletic in both BI and ML analyses albeit with moderate support (PP = 0.87/UFBS = 82), with three strongly supported and genetically well–differentiated clades. The first clade CI is comprised of all Oriental *Oocyclus* species, and is recovered as sister to the remaining taxa. The two other clades CII and CIII are respectively comprised of all South Indian/Sri Lankan and Neotropical species. *Ophthalmocyclus* is found nested within the Indian clade with strong support.

3.2. Divergence time estimates

All BEAST runs converged as indicated by ESS values above 200 for all parameters. The marginal likelihood calculations obtained via stepping–stone sampling are given in Table S7. The run receiving the best marginal likelihood (SSML = −162587.1163) was set using the maximum age of the stem Hydrophiloidea (273 Myr), 5 partitions (one per gene fragment except for the mitochondrial gene fragments) and an exponential prior density for all fossil calibrations. Although we recover substantial differences in divergence time estimates for the root and to a lesser extent for the age of Hydrophilidae, our estimates are rather comparable for the crown *Oocyclus* and clades CI, CII and CIII (Fig. 3). The results of the BEAST dating analyses are summarized in Fig. 2 for the whole family under the best run as supported by marginal likelihood estimates. This analysis recovers an origin of *Oocyclus* in the mid–Cretaceous, 100.47 Ma (95% HPD: 87.98–114.16 Ma). We infer an age for the crown of the Oriental clade CI in the Paleocene, 60.64 Ma (95% HPD: 47.36–74.18 Ma). The crowns for the Indian and Neotropical clades CII and CIII are respectively dated from the Eocene, 52.26 Ma (95% HPD: 40.14–65.42 Ma), and from the Upper Cretaceous, 68.22 Ma (95% HPD: 58.29–78.63 Ma). The substitution rates of each gene fragment calculated in the best analysis are given in Table S8.

3.3. Biogeographic analyses

The different analyses conducted in BioGeoBEARS resulted in contrasting biogeographical patterns as summarized in Fig. 4 and Table 2 (see Figs. S3–S8 for more details). The analyses implying the founder–event jump dispersal parameter j received significantly better likelihoods than the models ignoring this parameter. The analyses based on the reduced topology (SS) and without an explicit model of range evolution (model M0) resulted mostly in a pattern invoking a Pangean origin of *Oocyclus*, with a widespread ancestral disjunct distribution. The overall best analysis under model M0 (M0 SS DIVALIKE +j, LnL = −55.50) recovered an origin of *Oocyclus* in the Andes, India and Oriental region, followed by multiple vicariant events. The analyses based on the topology including outgroups (SL) but without an explicit model of range evolution (M0) resulted in very different patterns depending on the inclusion of the j parameter. The best analysis (M0 SL DIVALIKE+j, LnL = −67.27) recovered an origin of *Oocyclus* in the Oriental region, followed by transoceanic dispersal toward India in the Upper Cretaceous, and a colonization of the Andes out of India at the end of the Cretaceous. The analyses performed based on the topology including outgroups (SL) or excluding them (SS), and with an explicit model of range evolution (models M1 or M2) estimated very similar patterns (Table 2). All analyses based on the reduced topology (SS) and with an explicit model of range evolution (M1 or M2) recovered a Gondwanan scenario (except the M2 SS DEC+j, LnL = −55.09 with a Laurasian scenario). The overall best analysis (M1 SS DIVALIKE+j, LnL = −52.38) recovered a widespread disjunct ancestral range in the Guiana Shield and India, followed by a colonization of the Oriental region via dispersal and several vicariant events. The analyses based on the topology including outgroups (SL) and with an explicit model of range evolution (M1 or M2) resulted in different patterns depending on the inclusion of the j parameter. When included, all analyses recovered a Laurasian origin in the Oriental region, whereas when omitted, all analyses recovered a Gondwanan origin. The best analysis (M1 SL DEC+j, LnL = −60.56), recovered an origin of *Oocyclus* in the Oriental region, followed by transoceanic dispersal toward India in the Upper Cretaceous, and another transoceanic dispersal event toward the Guiana Shield at the end of the Cretaceous. In the first three best analyses described above, the relative probability of the most likely

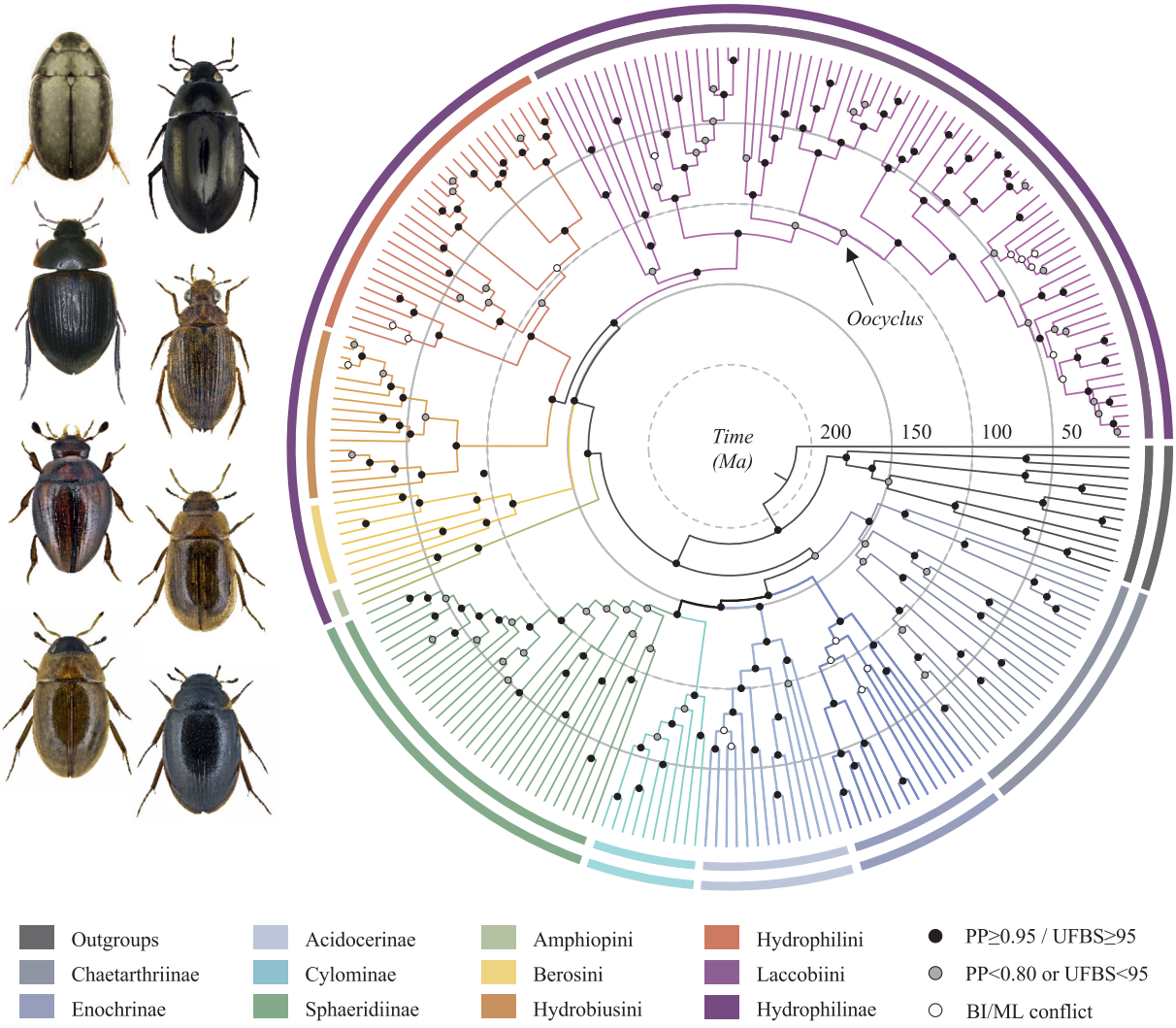

Fig. 2. Molecular phylogeny and divergence time estimates of the family Hydrophilidae Circular timetree of Hydrophilidae inferred in BEAST. This chronogram is derived from the best BEAST analysis as selected using marginal likelihoods (see Results). All major clades are color-coded as indicated in the inserted caption. Nodal support values form the MrBayes (posterior probabilities, PP) and IQ-TREE (ultrafast bootstraps, UFBS) analyses are given according to the inserted caption. Pictures (credit Udo Schmidt) from top to bottom; *Scoliopsis* sp. (Laccobiini), *Sternolophus inconspicuous* (Hydrophilini), *Hydrocassis scapulata* (Hydrobiusini), *Berosus incretus* (Berosini), *Pachysternum nigrovittatum* (Sphaeridiinae), *Helochares pallens* (Acidocerinae), *Enochrus esuriens* (Enochrinae), *Crenitis punctatostriata* (Chaetarthriinae).

ancestral ranges was low for the initial nodes of the backbone. In the last one however, the relative probability of the ancestral ranges was very high for all nodes across the topology. We present the detailed biogeographical pattern of this latter analysis in Fig. 5.

3.4. Diversification dynamics

The results of the TreePar analyses are provided in Tables S9 and S10. The analysis conducted on the reduced topology (SS) recovered a unique shift in diversification in the late Miocene (8Ma) with a decrease in the rate of diversification. The analysis conducted with the topology including outgroups recovered a model without rate shifts as the best, therefore assuming a constant diversification rate for the evolution of the clade. The BAMM analyses converged well with ESS values above 1000 both for the log-likelihood and the number of shift events (Fig. S7 and S8). The analyses conducted with the SL and SS chronograms recovered a unique shift configuration within the 95% credible set of configurations. The associated pattern included no rate shift across the phylogeny, and a declining speciation rate through timer (see Figs. S7 and S8).

Table 1
Results of the topological tests conducted in IQ-TREE.

Tree	logL	deltaL	bp-RELL	p-KH	p-SH	c-ELW	p-AU
Paraphyly	−159371.767	0.000	0.5690 +	0.5600	1.0000	0.5680	0.5618
Monophyly	−159376.134	4.367	0.4310 +	0.4400	0.4400	0.4320	0.4382

deltaL, logL difference from the maximal logl in the set; bp-RELL, bootstrap proportion using RELL method (Kishino et al., 1990); p-KH, p-value of one sided Kishino-Hasegawa test (1989); p-SH, p-value of Shimodaira-Hasegawa test (1999); c-ELW, Expected Likelihood Weight (Strimmer & Rambaut, 2002); p-AU, p-value of approximately unbiased (AU) test (Shimodaira, 2002). Plus signs denote the 95% confidence sets. All tests performed 1000 resampling using the RELL method.

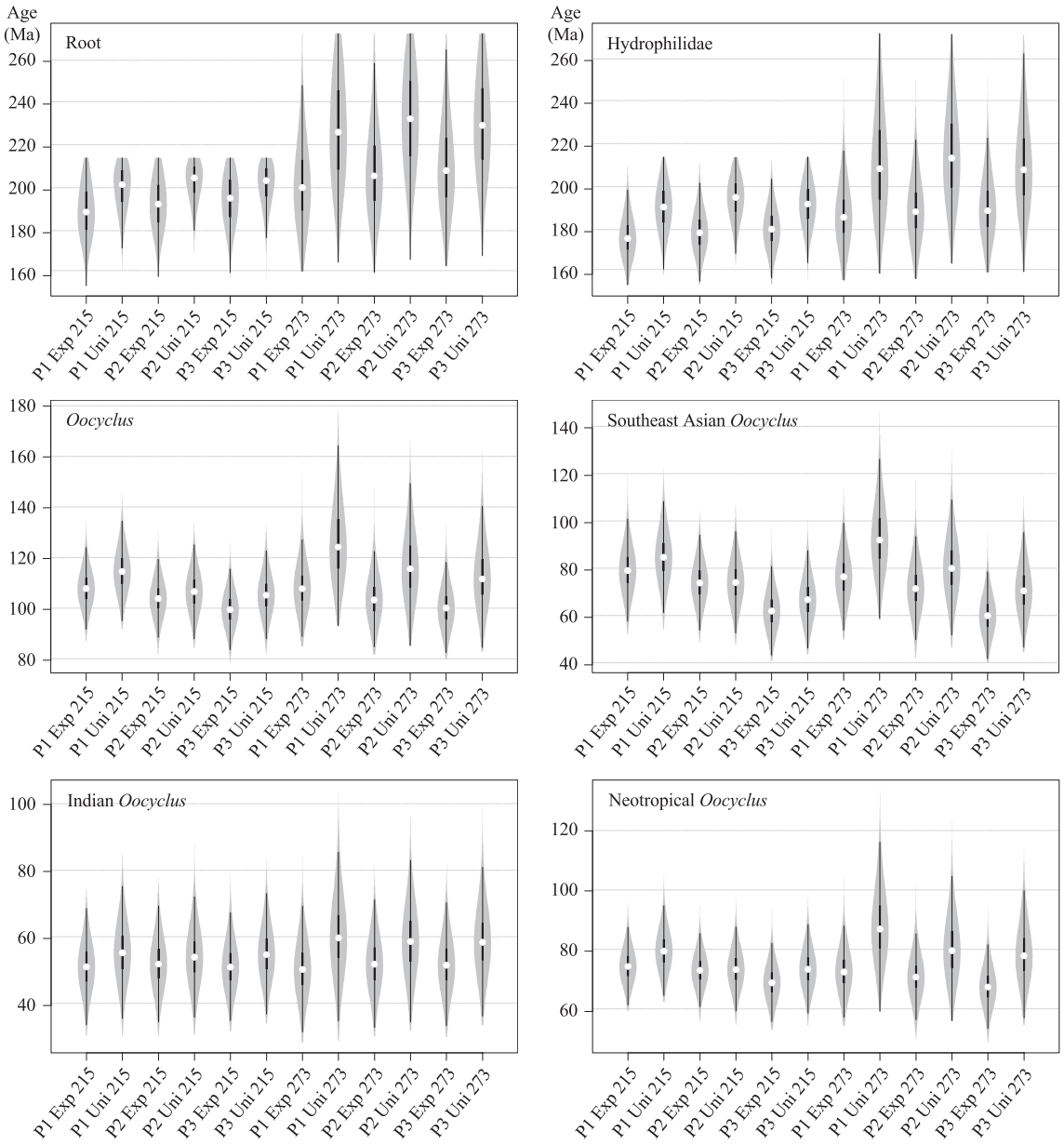

Fig. 3. BEAST divergence times estimates under different priors Violin plots presenting mean ages (white dots) along with the posterior distribution (grey area) of the 95% credibility intervals (black bars) inferred in the different BEAST analyses. P1, one relaxed molecular clock for the mitochondrial gene fragments and one partition for the nuclear gene fragments; P2, one relaxed molecular clock for the ribosomal gene fragments, one relaxed molecular clock for the nuclear protein-coding gene fragments, and one relaxed molecular clock for the mitochondrial gene fragments; P3, one relaxed molecular clock per nuclear gene fragment and one relaxed molecular clock for all mitochondrial gene fragments; Exp, fossil exponential prior distribution; Uni, fossil uniform prior distribution; 215, maximum age corresponding to the crown median age of Hydrophiloidea in Toussaint et al. (2017c); 273, maximum age corresponding to the crown median age of Hydrophiloidea in Toussaint et al. (2017c).

4. Discussion

4.1. Systematics of Laccobiini

The phylogenetic placement of the tribe Laccobiini and monophyly of the genus *Oocyclus* have remained uncertain after recent studies (Short & Fikáček, 2013; Toussaint et al., 2016). Short & Fikáček (2013) suggested that the tribe Laccobiini was paraphyletic due to the placement of the *Paracymus*-group as sister to the tribes Hydrobiusini and Hydrophilini. They also inferred *Oocyclus* nested within the *Laccobius*-group, and as paraphyletic due to the placement of clade CI as sister to the genera *Arabhydrus*, *Hydrophilomima* and *Pelthydrus*. In Toussaint et al. (2016), *Oocyclus* was recovered as paraphyletic as in Short & Fikáček (2013), but Laccobiini was recovered as monophyletic. Reduced taxonomic and genetic sampling in these two previous studies might have hampered the phylogenetic resolution in the tribe Laccobiini. Using a more comprehensive dataset, our analyses recover a monophyletic Laccobiini, which is congruent with Toussaint et al. (2016) though in contrast to Short & Fikáček (2013) in which the *Laccobius*–group and *Paracymus*–group were found to be paraphyletic with weak support. This is likely due to significantly increased taxon sampling, as our analysis includes four times as many species of the tribe than the earlier works. Within the *Laccobius*–group, our analysis differs in two notable ways that also seem likely due to increased taxon sampling. First, we recover a monophyletic *Oocyclus* while prior studies had found the genus to be paraphyletic (Short & Fikáček, 2013; Toussaint et al., 2016). Specifically, the Southeast Asian taxa in clade CI were previously found to be sister to

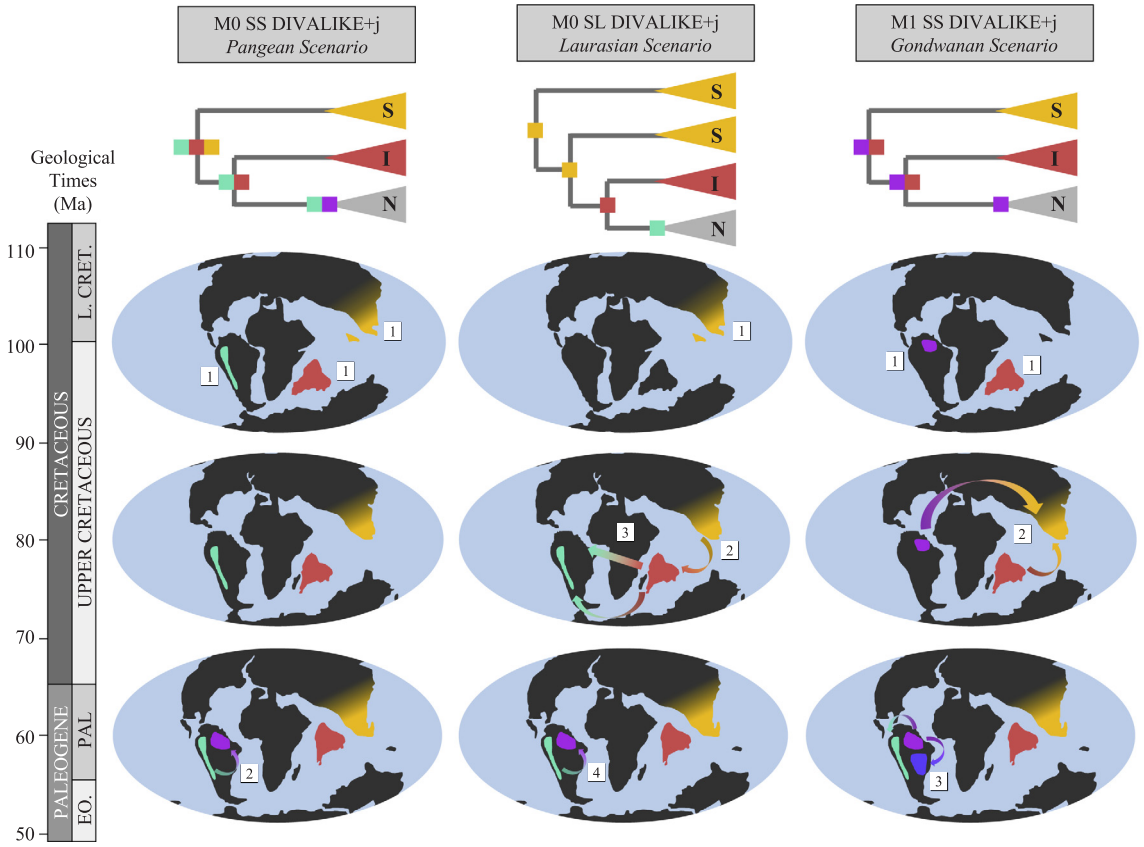

Fig. 4. BioGeoBEARS biogeographical scenarios as estimated under different models and topologies Summary of the biogeographical scenarios derived from the best BioGeoBEARS models with M0 (SS and SL) and M1 (SS). Schematic phylogenetic trees are presented to summarize the relationships inferred among the three main clades (CI, CII and CIII) of the genus *Oocyclus*. The color-coding in the phylogenetic trees follows the one used for the regions in the different maps. The numbered white squares indicate the synchronicity or chronological ordering of biogeographical events. Schematic reconstructions of landmass positions 100, 80 and 40 Ma following Seton et al. (2012) are presented.

(*Arabhydrus* + *Pelthydrus* + *Hydrophilomima*), which were together sister to the remaining *Oocyclus*. This study includes a substantially larger sampling of *Oocyclus* diversity that may have caused the resolution of the genus as monophyletic (but see Table 1 regarding the topological tests conducted). The genus is morphologically well-defined and no characters are known which would hint towards the genus not being monophyletic. Second, the genus *Pelthydrus* is shown to be paraphyletic; prior studies had only included a single exemplar. The genus is composed of two morphologically distinct subgenera, *Pelthydrus* (*sensu stricto*) and *Globipelthydrus*. Our analyses resolve each of these subgenera as monophyletic, but the genus as paraphyletic with respect to *Arabhydrus* and *Hydrophilomima* (Fig. 1). Additional sampling within *Pelthydrus* would be desirable before making taxonomic changes to the genus. As all representatives of all three genera occur in the Southeast Asia and one on the Arabian Peninsula, the internal relationships of the group do not affect the biogeographic reconstructions within *Oocyclus*.

4.2. Notes on the importance of comparative macroevolutionary analyses

Our dating analyses yielded rather similar ages for the various clades within *Oocyclus* (Fig. 3), therefore we believe our biogeographical estimations are unlikely to be biased by divergence time estimation uncertainty. However, the dating analyses recover very different ages in other parts of the hydrophiloid tree, illustrating that partitioning strategies, prior densities applied to fossil calibrations, and more importantly choice of maximum ages need to be tested in a comparative framework to assess the robustness of inferred timeframes (e.g. Warnock et al., 2015).

Our analyses of ancestral range estimation recovered very different patterns depending on the topology considered (SS vs. SL), implementation of the founder–event jump dispersal parameter j, or use of an explicit model of range evolution based on time–dependent adjacency matrices and dispersal rate scalers. Overall, we find that the use of an explicit model of range evolution results in improved likelihoods for both topologies (SS and SL). We argue a biogeographical model that considers the arrangement of areas and their tectonic evolution through time is biologically more tenable than a model assuming equal dispersal rates between adjacent and remote areas, between areas that were not extant throughout the age of the lineage, or among those that have substantially changed position or size during the evolution of the group. Considering this and the improvement in likelihood when using a designed model, we choose not to discuss in detail the two series of analyses based on a null model M0. The two remaining series of analyses recover divergent patterns of range evolution depending on the topology considered (Table 2). The best analysis of each series is summarized in Fig. 4. Broadly, we recover a Laurasian origin when including outgroups of *Oocyclus*, but a Gondwanan origin when excluding them. The analysis based on the chronogram excluding outgroups supports a scenario where the ancestor of *Oocyclus* would have been distributed in India and in the Guiana Shield. These two regions, in the mid–Cretaceous, were extremely distant from each other, being separated by Africa and multiple oceanic barriers (Seton et al., 2012). As a result, this scenario would also require regional extinction at least in Africa to explain the disjunct distribution of *Oocyclus* in the mid-Cretaceous. This is not an impossible evolutionary history, and maybe *Oocyclus* beetles existed at some point in Africa. Based on the extensive amount of work that has been conducted in Africa by water beetle

Table 2
Detailed results of the BioGeoBEARS analyses.

Model	LnL	P.	d	e	j	Ak. W.	N0	N1	N2	N3	N4	N5	N6	N7	Origin
M0 SS DEC	−64.63219	2	0.00084	0.00000	0.00000	0.00029	–	GIS	S*	AGI	I*	AG*	G*	A*	Pangea
M0 SS DEC+j	−69.97148	3	0.00053	0.00834	0.01721	0.00000	–	AIS	S*	AI	I*	A	G*	A*	Pangea
M0 SS DIVALIKE	−65.04566	2	0.00121	0.00000	0.00000	0.00019	–	AIS	S*	AGI	I*	AG	GB*	A*	Pangea
M0 SS DIVALIKE+j	**−55.49513**	**3**	**0.00031**	**0.00000**	**0.02109**	**0.99339**	**–**	**AIS**	**S***	**AI**	**I***	**AG**	**G***	**A***	**Pangea**
M0 SS BAYAREALIKE	−83.20432	2	0.00079	0.00852	0.00000	0.00000	–	AIS	S*	AI	I*	AG	GB	A*	Pangea
M0 SS BAYAREALIKE+j	−60.58433	3	0.00023	0.00140	0.01901	0.00612	–	CG	S*	CG	I*	CG	G*	A*	Pangea
M0 SL DEC	−76.39707	2	0.00075	0.00000	0.00000	0.00029	GIS	GIS	S*	AGI	I*	AG*	G*	A*	Pangea
M0 SL DEC+j	−70.93029	3	0.00020	0.00000	0.05356	0.02493	S	S	S*	I	I*	A	G*	A*	Laurasia
M0 SL DIVALIKE	−80.02460	2	0.00097	0.00000	0.00000	0.00001	AIS	AIS	S*	AGI	I*	AG	GB*	A*	Pangea
M0 SL DIVALIKE+j	**−67.26627**	**3**	**0.00020**	**0.00000**	**0.02032**	**0.97262**	**S**	**S**	**S***	**I**	**I***	**A**	**G***	**A***	**Laurasia**
M0 SL BAYAREALIKE	−96.63823	2	0.00060	0.00808	0.00000	0.00000	AIS	AIS	S*	AI	I*	AG	GB	A*	Pangea
M0 SL BAYAREALIKE+j	−73.37805	3	0.00017	0.00055	0.00526	0.00216	CG	CG	S*	CG	I*	CG	G	A	Gondwana
M1 SS DEC	−74.95865	2	0.00279	0.00209	0.00000	0.00000	–	GI	I*	GI	I*	AGB	GB*	A*	Gondwana
M1 SS DEC+j	−56.88273	3	0.00097	0.00000	0.01347	0.01006	–	GI	S*	GI	I*	G	G*	A*	Gondwana
M1 SS DIVALIKE	−80.03862	2	0.00396	0.00529	0.00000	0.00000	–	I*	I*	GI	I*	AGB	GB*	A*	Gondwana
M1 SS DIVALIKE+j	**−52.38286**	**3**	**0.00077**	**0.00000**	**0.04495**	**0.90574**	**–**	**GI**	**S***	**GI**	**I***	**G**	**G***	**A***	**Gondwana**
M1 SS BAYAREALIKE	−90.66567	2	0.00280	0.00938	0.00000	0.00000	–	GI	I*	GI	I*	G	GB*	A*	Gondwana
M1 SS BAYAREALIKE+j	−54.75842	3	0.00045	0.00048	0.02982	0.08420	–	CG	S*	CG	I*	CG	G*	A*	Gondwana
M1 SL DEC	−101.91475	2	0.00387	0.00433	0.00000	0.00000	I	I	I*	GI*	I*	AG	GB*	A*	Gondwana
M1 SL DEC+j	**−60.56373**	**3**	**0.00054**	**0.00000**	**0.04547**	**0.55185**	**S***	**S***	**S***	**I***	**I***	**G**	**G***	**A***	**Laurasia**
M1 SL DIVALIKE	−104.21122	2	0.00478	0.00384	0.00000	0.00000	I*	I*	I*	GI*	I*	AG	GB*	A*	Gondwana
M1 SL DIVALIKE+j	−60.83358	3	0.00065	0.00000	0.04843	0.42133	S*	S*	S*	I*	I*	G	G*	A*	Laurasia
M1 SL BAYAREALIKE	−115.66614	2	0.00390	0.01018	0.00000	0.00000	I	I*	I	GI	I*	G	GB	A*	Gondwana
M1 SL BAYAREALIKE+j	−63.58783	3	0.00114	0.00011	0.03499	0.02682	S*	S*	S*	I*	I*	G	G*	A*	Laurasia
M2 SS DEC	−75.08251	2	0.00277	0.00210	0.00000	0.00000	–	GI	I*	GI	I*	AGB	GB*	A*	Gondwana
M2 SS DEC+J	−55.08997	3	0.00076	0.00000	0.08724	0.07583	–	S	S*	I	I*	G	G*	A*	Laurasia
M2 SS DIVALIKE	−80.01872	2	0.00390	0.00534	0.00000	0.00000	–	I*	I*	GI	I*	AGB	GB*	A*	Gondwana
M2 SS DIVALIKE+J	**−52.63423**	**3**	**0.00074**	**0.00000**	**0.04703**	**0.88379**	**–**	**GI**	**S***	**GI**	**I***	**G**	**G***	**A***	**Gondwana**
M2 SS BAYAREALIKE	−90.81965	2	0.00276	0.00933	0.00000	0.00000	–	GI	I*	GI*	I*	G	GB	A*	Gondwana
M2 SS BAYAREALIKE+J	−55.72023	3	0.00084	0.00091	0.02374	0.04038	–	CG	S*	CG	I*	CG	C	A*	Gondwana
M2 SL DEC	−101.97547	2	0.00395	0.00434	0.00000	0.00000	I	I	I*	GI*	I*	AG	GB	A*	Gondwana
M2 SL DEC+J	**−61.78517**	**3**	**0.00055**	**0.00000**	**0.04957**	**0.54281**	**S***	**S***	**S***	**I***	**I***	**A***	**G***	**A***	**Laurasia**
M2 SL DIVALIKE	−104.24774	2	0.00487	0.00394	0.00000	0.00000	I*	I*	I*	GI*	I*	AG	GB*	I*	Gondwana
M2 SL DIVALIKE+J	−61.96694	3	0.00071	0.00000	0.05184	0.45259	S*	S*	S*	I	I*	A	G*	A*	Laurasia
M2 SL BAYAREALIKE	−115.8453	2	0.00396	0.01022	0.00000	0.00000	I	I	I*	GI	I*	G	GB	A*	Gondwana
M2 SL BAYAREALIKE+J	−66.55416	3	0.00043	0.00024	0.02054	0.00461	S	S	S*	I	I*	A	G*	A*	Laurasia

LnL, log–likelihood of the model; P., number of parameters; d, dispersal parameter; e, extinction parameter; j, jump–dispersal founder event jump dispersal parameter; Ak. W., Akaike weight; M0, null unconstrained model; M1, model with designed adjacency and dispersal multiplier matrices; SS, *Oocyclus* topology sensu stricto; SL; *Oocyclus* topology with the sister clade comprising *Arabhydrus*, *Hydrophilomima* and *Pelthydrus*; A, Andes; B, Brazilian Shield; C, Central America; G; Guiana Shield; I; India/Sri Lanka; P, Arabian Peninsula; S, Oriental Region; Asterisks indicate a relative probability Rp > 50% for a given estimated ancestral range

specialists, it seems very unlikely that these beetles currently exist on this continent. Using a phylogeny of extant taxa and in the absence of *Oocyclus* fossils, it is difficult to favor one hypothesis over the other. Our BAMM and TreePar diversification rate analyses do not detect a general pattern of extinction across *Oocyclus*, lending more support for the dynamic biogeographic pattern over the regional extinction one. However estimating extinction from small phylogenies is always challenging, and BAMM and TreePar do not allow the detection of punctual extinction events across the phylogeny of *Oocyclus*, therefore patterns invoking extinction to explain the current distribution of *Oocyclus* beetles cannot be discarded. Overall, our suite of analyses showcases the importance of a comparative framework as opposed to a single biogeographic analysis that can often give a simplistic view of evolutionary trajectories. We also argue that broadening the taxon sampling to include immediate outgroups of taxa under the focus of biogeographic studies should be implemented when possible. Clearly, in the case of *Oocyclus*, as likely in many other clades for which the biogeographic history appears complex, the inclusion of outgroups provides a much more accurate estimation of ancestral ranges and can shed light on patterns that would otherwise be obscured by the lack of external information from the sister-lineages.

Finally, it is noteworthy that the use of the founder–event jump dispersal parameter j dramatically influences the biogeographic estimations in this clade and in many others. One should keep in mind that the inclusion of this parameter assumes very different processes and that all analyses, even the ones with apparently lower likelihoods in BioGeoBEARS can still be of interest when trying to elucidate the origins and range evolution of clades through time. In the case of *Oocyclus*, all models that did not include the j parameter supported an origin in a Pangean setting, implying either an even older widespread distribution across Pangea followed by multiple events of regional extinction, or an origin shaped by trans-Pangean long-distance dispersal events. We argue that these patterns although plausible are less likely than the ones (Gondwanan or Laurasian) estimated using the j parameter. Certainly a large-scale estimation of ancestral ranges across Hydrophilidae will help in the future shed light on the intricate evolution of *Oocyclus* beetles.

4.3. Broad-scale patterns of biogeographic evolution

The results of our dating and ancestral range estimations shed some light on the evolution of widespread ancient lineages. It has been notoriously difficult to untangle the diversification mechanisms in old lineages because understanding the evolution of landmass connectivity and locations through time is not trivial (e.g., Clouse et al., 2017). However, our results present an intriguing new pattern in Gondwanan-Laurasian biogeography. In this study, the pattern inferred when including outgroups recovers a Laurasian origin of *Oocyclus* in the mid–Cretaceous (Fig. 5). Under this scenario, the ancestor of the group would have been restricted to the Oriental region and later dispersed via long–distance dispersal (LDD) toward India. The LDD event toward India would have taken place in the Upper Cretaceous, when or soon after India separated from Gondwana (Seton et al., 2012). India split from Madagascar about 88 Ma (Gibbons et al., 2013) but remained

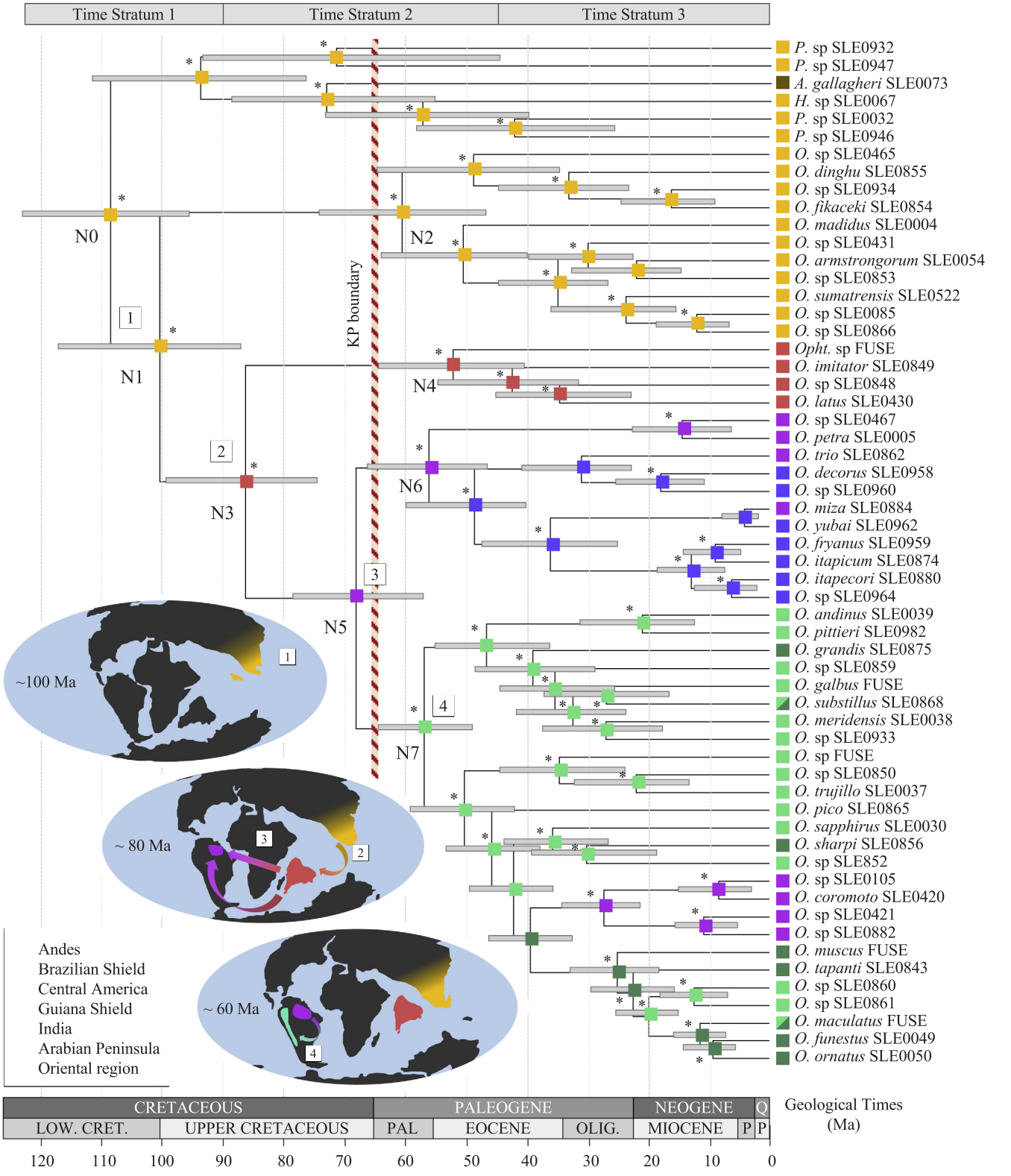

Fig. 5. BioGeoBEARS biogeographical scenario of the genus *Oocyclus* BEAST chronogram with median ages and 95% credibility intervals (horizontal grey bars) for each node of the genus *Oocyclus* and sister clade (SL chronogram). The biogeographical scenario as estimated using BioGeoBEARS with the preferred model including outgroups (M1 SL DEC+j, LnL = −60.56373; see Results) is presented. The distribution of all terminals in the areas defined in BioGeoBEARS are given with squares color-coded according to current geographical ranges and following the inserted caption. Asterisks indicate a relative probability of the ancestral geographical range above 50% (see Table 2 and Figs. S3–S6 for more details). The numbered white squares indicate the synchronicity or chronological ordering of biogeographical events. Schematic reconstructions of landmass positions 100, 80 and 40 Ma following Seton et al. (2012) are presented.

attached to Seychelles until the end of the Cretaceous about 63 Ma (Armitage et al., 2011). Although, to our knowledge, the directionality of this pattern is unique in the literature, such long–distance dispersal, in terms of distance, has been suggested in other groups of water beetles (e.g. Morinière et al., 2016; Toussaint et al., 2017b; Toussaint & Short, 2017). Indeed, several lineages have been suggested to have dispersed in the other direction, from Gondwana to Laurasia through the rafting Indian plate, a hypothesis coined the 'biotic ferry' (Hedges, 2003, see Datta-Roy and Karanth, 2009; Toussaint et al., 2016 for reviews and criticisms). In the case of *Oocyclus*, India acted more as a 'biotic hub', allowing the dispersal of these beetles from Laurasia toward Gondwana through stepping-stone long-distance dispersal. Although there is very little information regarding the dispersal capacity of *Oocyclus* beetles, adults have been observed to fly when removed from their hygropetric habitat, and are occasionally collected in flight intercept traps (Short and Toussaint, pers. obs.). Therefore, the LDD event supported by the DEC + j model does not seem unreasonable.

Following this early colonization of India, some lineages drifted along with the island as it moved toward Eurasia in the Paleocene. As suggested in other laccobiine beetles (*Scoliopsis*, Toussaint et al., 2016), as well as in a few other groups (e.g. Bossuyt & Milinkovitch, 2001; Pirie et al., 2015; but see Pyron, 2014 regarding the biogeography of frog lineages), this lineage would have had to cope with the extreme tectonic and volcanic activities triggered by the collision of the Indian and Asian plates (Chenet et al., 2008). As suggested for the cascade beetle genus *Scoliopsis*, the intense volcanism happening during the formation of the Deccan traps could have fortunately provided rock–-seep specialists such as *Oocyclus* beetles, with a variety of suitable habitats, therefore allowing the Indian lineages to survive until the final docking of India (Toussaint et al., 2016). This might be supported by the fact that lineage diversification in India only started after the landmass collided with Asia, allowing continental dispersal.

The lineage endemic to the Oriental region only started to diversify in the Paleocene, and did not manage to further colonize the Australian region despite the formation of the Wallacea in the Miocene (Hall, 2013). This is surprising as many lineages of insects that originated in the Oriental region took advantage of the geological re-assemblage of the Indo-Australian archipelago (IAA) to successfully colonize the Australian region from the north (e.g., Condamine et al., 2013; Mezger & Moreau, 2016; Morinière et al., 2016; Toussaint and Balke, 2016). *Oocyclus* is restricted to continental Asia in addition to some species distributed in the Greater Sunda Islands and Taiwan (Hansen, 1999), however, the genus is absent from the Australian region. As the Australian water beetle fauna is well–known, it is very unlikely that *Oocyclus* could have been overlooked in Australia and adjacent archipelagoes. Other seepage specialist genera within the Hydrophilidae (e.g. *Notionotus*) are also absent from this biogeographical region, but the cause for this pattern remains unknown.

Our biogeographical analysis suggests that the Guiana Shield was colonized through LDD from drifting India. This biogeographical pattern is the most puzzling, because it implies overland dispersal across Africa and eastern Neotropics as well as oceanic dispersal. This LDD event seems rather unlikely even though this is the most likely scenario under our estimation. There is also no other empirical evidence of such a LDD pattern. The transition from India to Neotropics therefore remains quite enigmatic. A possible alternative scenario would invoke dispersal from India through Antarctica and toward South America in the Upper Cretaceous. Examples of biogeographic patterns invoking a role of Antarctica have been suggested in several groups in the past (e.g., Kayaalp et al., 2013, 2017; Givnish et al., 2016; Gustafson & Miller, 2017; Toussaint & Short, 2017; Toussaint et al., 2017b). Although the existence of land bridges facilitating such dispersal events has been questioned (Ali and Aitchison, 2009; Ali and Krause, 2011), transoceanic dispersal would have been possible. However, without a better knowledge of the fossil record, it will not be possible to elucidate this rather unique pattern. After the colonization of the Guiana Shield where the lineage slowly diversified and later colonized the Brazilian Shield (Fig. 5), we reconstruct an early colonization of the Andes where the group started to diversify in the Paleogene (Fig. 5). Although the western Neotropics were characterized by subduction for the past 100 Myr (Cobbold et al., 2007), the Andes were not as rugged and high as since the Miocene (Mora et al., 2010). Therefore, colonization of the Andean region from the Guiana Shield would have only required continental dispersal over a rather uniform landscape. The later colonization of Central America and reverse colonization of Guiana Shield do not seem to match particular events in the geological history of the Neotropical region (Hoorn et al., 2010).

4.4. Conclusion

Our study suggests that biogeographic estimations/reconstructions should ideally be conducted in a comparative framework, to assess the impact of outgroup sampling, divergence time uncertainty and models of range evolution on estimated biogeographical scenarios. Using such a comprehensive set of likelihood analyses, we show that the historical biogeography of tropical cascade beetles in the genus *Oocyclus* is very complex. Our different analyses support various biogeographical scenarios, and the one we hypothesize to be the most likely implies transoceanic long distance dispersal between the Oriental region, India and the Neotropics. Such a unique scenario sheds light on the intricacy of ancient arthropod lineage biogeography with respect to the Earth landmass evolution throughout geological eras.

Acknowledgements

We thank the editor and anonymous reviewers for inisghtful comments on an earlier version of this manuscript. This study was funded by US National Science Foundation grant DEB-1453452 to AEZS.

Appendix A. Supplementary material

Supplementary data associated with this article can be found, in the online version, at https://doi.org/10.1016/j.ympev.2018.04.023.

References

Ali, J.R., Aitchison, J.C., 2009. Kerguelen Plateau and the Late Cretaceous southern-continent bioconnection hypothesis: tales from a topographical ocean. J. Biogeogr. 36 (9), 1778–1784.
Ali, J.R., Krause, D.W., 2011. Late Cretaceous bioconnections between Indo-Madagascar and Antarctica: refutation of the Gunnerus Ridge causeway hypothesis. J. Biogeogr. 38 (10), 1855–1872.
Armitage, J.J., Collier, J.S., Minshull, T.A., Henstock, T.J., 2011. Thin oceanic crust and flood basalts: India-Seychelles breakup. Geochem. Geophy. Geosy. 12(5).
Baca, S.M., Toussaint, E.F.A., Miller, K.B., Short, A.E., 2017. Molecular phylogeny of the aquatic beetle family Noteridae (Coleoptera: Adephaga) with an emphasis on data partitioning strategies. Mol. Phylogenet. Evol. 107, 282–292.
Baele, G., Lemey, P., Bedford, T., Rambaut, A., Suchard, M.A., Alekseyenko, A.V., 2012. Improving the accuracy of demographic and molecular clock model comparison while accommodating phylogenetic uncertainty. Mol. Biol. Evol. 29 (9), 2157–2167.
Beattie, R.G., Avery, S., 2012. Palaeoecology and palaeoenvironment of the Jurassic Talbragar Fossil Fish Bed, Gulgong, New South Wales, Australia. Alcheringa 36 (4), 453–468.
Berger, B.A., Kriebel, R., Spalink, D., Sytsma, K.J., 2016. Divergence times, historical biogeography, and shifts in speciation rates of Myrtales. Mol. Phylogenet. Evol. 95, 116–136.
Bernhard, D., Schmidt, C., Korte, A., Fritzsch, G., Beutel, R.G., 2006. From terrestrial to aquatic habitats and back again—molecular insights into the evolution and phylogeny of Hydrophiloidea (Coleoptera) using multigene analyses. Zool. Scripta 35 (6), 597–606.
Bilton, D.T., Toussaint, E.F., Turner, C.R., Balke, M., 2015. Capelatus prykei gen. et sp. n. (Coleoptera: Dytiscidae: Copelatinae)–a phylogenetically isolated diving beetle from the Western Cape of South Africa. Syst. Entomol. 40 (3), 520–531.
Bloom, D.D., Fikáček, M., Short, A.E., 2014. Clade age and diversification rate variation explain disparity in species richness among water scavenger beetle (Hydrophilidae) lineages. PLoS One 9 (6), 98430.
Bossuyt, F., Milinkovitch, M.C., 2001. Amphibians as indicators of early tertiary" out–of–India" dispersal of vertebrates. Science 292 (5514), 93–95.
Buffon, M.D., 1769. Histoire naturelle générale et particulière des animaux. Imprimerie

royale. Paris: Panckouche éd.
Cai, L., Xi, Z., Peterson, K., Rushworth, C., Beaulieu, J., Davis, C.C., 2016. Phylogeny of Elatinaceae and the tropical Gondwanan origin of the Centroplacaceae (Malpighiaceae, Elatinaceae) Clade. PloS One 11 (9), 0161881.
Chenet, A.L., Fluteau, F., Courtillot, V., Gérard, M., Subbarao, K.V., 2008. Determination of rapid Deccan eruptions across the Cretaceous-Tertiary boundary using paleomagnetic secular variation: Results from a 1200-m-thick section in the Mahabaleshwar escarpment. J. Geophys. Res. B: Solid Earth 113 (B4).
Clouse, R.M., Branstetter, M.G., Buenavente, P., Crowley, L.M., Czekanski-Moir, J., General, D.E.M., Giribet, G., Harvey, M.S., Janies, D.A., Mohagan, A.B., Mohagan, D.P., 2017. First global molecular phylogeny and biogeographical analysis of two arachnid orders (Schizomida and Uropygi) supports a tropical Pangean origin and mid-Cretaceous diversification. J. Biogeogr. 44 (11), 2660–2672.
Cobbold, P.R., Rossello, E.A., Roperch, P., Arriagada, C., Gómez, L.A., Lima, C., 2007. Distribution, timing, and causes of Andean deformation across South America. Geolog. Soc., London, Special Publications 272 (1), 321–343.
Condamine, F.L., Toussaint, E.F.A., Cotton, A.M., Genson, G.S., Sperling, F.A., Kergoat, G.J., 2013. Fine-scale biogeographical and temporal diversification processes of peacock swallowtails (Papilio subgenus Achillides) in the Indo-Australian Archipelago. Cladistics 29 (1), 88–111.
Cox, C.B., Moore, P.D., 2010. Biogeography: An Ecological and Evolutionary Approach, eighth ed. Oxford, Blackwell Scientific Publications.
Darwin, C. 1859. On the origin of the species by natural selection. Murray.
Datta-Roy, A., Karanth, K. Praveen, 2009. The Out-of-India hypothesis: what do molecules suggest? J. Biosci. 34 (5), 687–697.
De Queiroz, A., 2005. The resurrection of oceanic dispersal in historical biogeography. Trends Ecol. Evol. 20 (2), 68–73.
Drummond, A.J., Suchard, M.A., Xie, D., Rambaut, A., 2012. Bayesian phylogenetics with BEAUti and the BEAST 1.7. Mol. Biol. Evol. 29 (8), 1969–1973.
Duchêne, S., Molak, M., Ho, S.Y., 2013. ClockstaR: choosing the number of relaxed–clock models in molecular phylogenetic analysis. Bioinformatics 30 (7), 1017–1019.
Eberle, J., Fabrizi, S., Lago, P., Ahrens, D., 2017. A historical biogeography of megadiverse Sericini—another story "out of Africa"? Cladistics 33 (2), 183–197.
Edgar, R.C., 2004. MUSCLE: multiple sequence alignment with high accuracy and high throughput. Nucl. Acids Res. 32 (5), 1792–1797.
Evanoff, E., McIntosh, W.C., Murphey, P.C., 2001 Stratigraphic Summary and 40Ar/39Ar Geocrhonology of the Florissant Formation, Colorado. In: Evanoff, E., Gregory-Wodzicki, K.M., Johnson, K.R. (Eds.), Fossil Flora and Stratigraphy of the Florissant Formation, Colorado.
Fikáček, M., Engel, M.S., 2011. An aquatic water scavenger beetle in Early Miocene amber from the Dominican Republic (Coleoptera: Hydrophilidae). Ann. Zool. Fenn. 61 (4), 621–628.
Fikáček, M., Schmied, H., Prokop, J., 2010a. Fossil hydrophilid beetles (Coleoptera: Hydrophilidae) of the Late Oligocene Rott Formation (Germany). Acta Geol. Sin. 84 (4), 732.
Fikáček, M., Prokop, J., Nel, A., 2010b. Fossil water scavenger beetles of the subtribe Hydrobiusina (Coleoptera: Hydrophilidae) from the Late Oligocene locality of Aix-en-Provence (France). Acta Entomol. Mus. Natl. Pragae 50, 445–458.
Fikáček, M., Prokin, A., Angus, R.B., Ponomarenko, A., Yue, Y., Ren, D., Prokop, J., 2012a. Phylogeny and the fossil record of the Helophoridae reveal Jurassic origin of extant hydrophiloid lineages (Coleoptera: Polyphaga). Syst. Entomol. 37 (3), 420–447.
Fikáček, M., Prokin, A.A., Angus, R.B., Ponomarenko, A.G., Yue, Y., Ren, D., Prokop, J., 2012b. Revision of Mesozoic fossils of the helophorid lineage of the superfamily Hydrophiloidea (Coleoptera: Polyphaga). Acta Entomol. Mus. Natl. Pragae 52 (1), 89–127.
Fikáček, M., Prokin, A., Yan, E., Yue, Y., Wang, B., Ren, D., Beattie, R., 2014. Modern hydrophilid clades present and widespread in the Late Jurassic and Early Cretaceous (Coleoptera: Hydrophiloidea: Hydrophilidae). Zool. J. Linn. Soc. 170 (4), 710–734.
Gamble, T., Bauer, A.M., Greenbaum, E., Jackman, T.R., 2008. Evidence for Gondwanan vicariance in an ancient clade of gecko lizards. J. Biogeogr. 35 (1), 88–104.
Gibbons, A.D., Whittaker, J.M., Müller, R.D., 2013. The breakup of East Gondwana: assimilating constraints from Cretaceous ocean basins around India into a best-fit tectonic model. J. Geophys. Res. B: Solid Earth 118 (3), 808–822.
Givnish, T.J., Zuluaga, A., Marques, I., Lam, V.K., Gomez, M.S., Iles, W.J., Ames, M., Spalink, D., Moeller, J.R., Briggs, B.G., Lyon, S.P., 2016. Phylogenomics and historical biogeography of the monocot order Liliales: out of Australia and through Antarctica. Cladistics 32 (6), 581–605.
Gustafson, G.T., Miller, K.B., 2017. Systematics and evolution of the whirligig beetle tribe Dineutini (Coleoptera: Gyrinidae: Gyrininae). Zool. J. Linn. Soc. 181 (1), 118–150.
Hall, R., 2013. The palaeogeography of Sundaland and Wallacea since the Late Jurassic. J. Limnol. 72 (s2), 1.
Hansen, M., 1999. World catalogue of insects. Volume 2: Hydrophiloidea (s. str.) (Coleoptera). Apollo Books.
Hedges, S.B., 2003. Biogeography: the coelacanth of frogs. Nature 425 (6959), 669–670.
Ho, S.Y., Phillips, M.J., 2009. Accounting for calibration uncertainty in phylogenetic estimation of evolutionary divergence times. Syst. Biol. 58 (3), 367–380.
Hoorn, C., Wesselingh, F.P., Ter Steege, H., Bermudez, M.A., Mora, A., Sevink, J., Sanmartín, I., Sanchez-Meseguer, A., Anderson, C.L., Figueiredo, J.P., Jaramillo, C., 2010. Amazonia through time: Andean uplift, climate change, landscape evolution, and biodiversity. Science 330 (6006), 927–931.
Huelsenbeck, J.P., Larget, B., Alfaro, M.E., 2004. Bayesian phylogenetic model selection using reversible jump Markov chain Monte Carlo. Mol. Biol. Evol. 21 (6), 1123–1133.
Hunt, T., Bergsten, J., Levkanicova, Z., Papadopoulou, A., John, O.S., Wild, R., Hammond, P.M., Ahrens, D., Balke, M., Caterino, M.S., Gómez-Zurita, J., 2007. A comprehensive phylogeny of beetles reveals the evolutionary origins of a superradiation. Science 318 (5858), 1913–1916.
Iturralde-Vinent, M.A., MacPhee, R.D.E., 1996. Age and paleogeographical origin of Dominican amber. Science 273, 1850–1852.
Katoh, K., Standley, D.M., 2013. MAFFT multiple sequence alignment software version 7: improvements in performance and usability. Mol. Biol. Evol. 30 (4), 772–780.
Kayaalp, P., Schwarz, M.P., Stevens, M.I., 2013. Rapid diversification in Australia and two dispersals out of Australia in the globally distributed bee genus, *Hylaeus* (Colletidae: Hylaeinae). Mol. Phylogenet. Evol. 66 (3), 668–678.
Kayaalp, P., Stevens, M.I., Schwarz, M.P., 2017. 'Back to Africa': increased taxon sampling confirms a problematic Australia-to-Africa bee dispersal event in the Eocene. Syst. Entomol. 42 (4), 724–733.
Kim, S.I., Farrell, B.D., 2015. Phylogeny of world stag beetles (Coleoptera: Lucanidae) reveals a Gondwanan origin of Darwin's stag beetle. Mol. Phylogenet. Evol. 86, 35–48.
Kishino, H., Hasegawa, M., 1989. Evaluation of the maximum likelihood estimate of the evolutionary tree topologies from DNA sequence data, and the branching order in Hominoidea. J. Mol. Evol. 29 (2), 170–179.
Kishino, H., Miyata, T., Hasegawa, M., 1990. Maximum likelihood inference of protein phylogeny and the origin of chloroplasts. J. Mol. Evol. 31 (2), 151–160.
Kosmowska-Ceranowicz, B., 1987. Charakterystyka mineralogiczno-petrograficzna bursztynonosnych osadów Eocenu w okolicach ChlÙpowo oraz osadów Paleogenu PolÙnocnej Polski. Biuletyn Instytutu Geologicznego 356, 29–50.
Kosmowska-Ceranowicz, B., Müller, C., 1985. Lithology and calcareous nannoplankton in amberbearing Tertiary sediments from boreholes Chłapowo (Northern Poland). Bull. Pol. Ac. Earth Sc. 33 (3–4), 119–129.
Kubisz, D., 2000. Fossil beetles (Coleoptera) from Baltic amber in the collection of the Museum of Natural History of ISEA in Krakow. Pol. Pis. Entomol. 2 (69), 225–230.
Kumar, S., Stecher, G., Tamura, K., 2016. MEGA7: Molecular Evolutionary Genetics Analysis version 7.0 for bigger datasets. Mol. Biol. Evol. 33 (7), 1870–1874.
Landis, M.J., Matzke, N.J., Moore, B.R., Huelsenbeck, J.P., 2013. Bayesian analysis of biogeography when the number of areas is large. Syst. Biol. 62 (6), 789–804.
Lanfear, R., Frandsen, P.B., Wright, A.M., Senfeld, T., Calcott, B., 2017. PartitionFinder 2: new methods for selecting partitioned models of evolution for molecular and morphological phylogenetic analyses. Mol. Biol. Evol. 34 (3), 772–773.
Lomolino, M.V., Brown, J.H., Sax, D.F., 2010. Island biogeography theory: Reticulations and reintegration of a biogeography of the species. In: Losos, J.B., Ricklefs, R.E. (Eds.), The theory of island biogeography revisited. Princeton, Princeton University Press 13 51.
Luebert, F., Couvreur, T.L., Gottschling, M., Hilger, H.H., Miller, J.S., Weigend, M., 2017. Historical biogeography of Boraginales: West Gondwanan vicariance followed by long-distance dispersal? J. Biogeogr. 44 (1), 158–169.
Mao, K., Milne, R.I., Zhang, L., Peng, Y., Liu, J., Thomas, P., Mill, R.R., Renner, S.S., 2012. Distribution of living Cupressaceae reflects the breakup of Pangea. Proc. Natl. Acad. Sci. USA 109 (20), 7793–7798.
Matzke, N.J., 2013. BioGeoBEARS: biogeography with Bayesian (and likelihood) evolutionary analysis in R scripts. R package, version 0.2, 1.
Matzke, N.J., 2014. Model selection in historical biogeography reveals that founder–event speciation is a crucial process in island clades. Syst. Biol. 63 (6), 951–970.
Mckenna, D.D., Wild, A.L., Kanda, K., Bellamy, C.L., Beutel, R.G., Caterino, M.S., Farnum, C.W., Hawks, D.C., Ivie, M.A., Jameson, M.L., Leschen, R.A., 2015. The beetle tree of life reveals that Coleoptera survived end-Permian mass extinction to diversify during the Cretaceous terrestrial revolution. Syst. Entomol. 40 (4), 835–880.
Mennes, C.B., Lam, V.K., Rudall, P.J., Lyon, S.P., Graham, S.W., Smets, E.F., Merckx, V.S., 2015. Ancient Gondwana break-up explains the distribution of the mycoheterotrophic family Corsiaceae (Liliales). J. Biogeogr. 42 (6), 1123–1136.
Mertz, D.F., Renne, P.R., 2005. A numerical age for the Messel fossil deposit (UNESCO World Heritage Site) derived from 40Ar/39Ar dating on a basaltic rock fragment. Cour. Forsch. Inst. Senckenberg 255, 67–75.
Mezger, D., Moreau, C.S., 2016. Out of South-East Asia: phylogeny and biogeography of the spiny ant genus *Polyrhachis* Smith (Hymenoptera: Formicidae). Syst. Entomol. 41 (2), 369–378.
Miller, M.A., Pfeiffer, W., Schwartz, T., 2010, November. Creating the CIPRES Science Gateway for inference of large phylogenetic trees. In: Gateway Computing Environments Workshop (GCE), 2010, 1–8.
Milner, M.L., Weston, P.H., Rossetto, M., Crisp, M.D., 2015. Biogeography of the Gondwanan genus Lomatia (Proteaceae), vicariance at continental and intercontinental scales. J. Biogeogr. 42 (12), 2440–2451.
Minh, B.Q., Nguyen, M.A.T., von Haeseler, A., 2013. Ultrafast approximation for phylogenetic bootstrap. Mol. Biol. Evol. 30 (5), 1188–1195.
Moore, B.R., Höhna, S., May, M.R., Rannala, B., Huelsenbeck, J.P., 2016. Critically evaluating the theory and performance of Bayesian analysis of macroevolutionary mixtures. Proc. Natl. Acad. Sci. USA 113 (34), 9569–9574.
Mora, A., Baby, P., Roddaz, M., Parra, M., Brusset, S., Hermoza, W., Espurt, N., 2010. Tectonic history of the Andes and sub–Andean zones: implications for the development of the Amazon drainage basin. Amazonia, Landscape and Species Evolution: A Look into the Past. Blackwell–Wiley, Hoboken, 38–60.
Morinière, J., Van Dam, M.H., Hawlitschek, O., Bergsten, J., Michat, M.C., Hendrich, L., Ribera, I., Toussaint, E.F.A., Balke, M., 2016. Phylogenetic niche conservatism explains an inverse latitudinal diversity gradient in freshwater arthropods. Sci. Reports 6, 26340.
Murienne, J., Daniels, S.R., Buckley, T.R., Mayer, G., Giribet, G., 2014. A living fossil tale of Pangaean biogeography. Proc. R. Soc. B 281 (1775), 20132648.
Nguyen, L.T., Schmidt, H.A., von Haeseler, A., Minh, B.Q., 2015. IQ–TREE: a fast and effective stochastic algorithm for estimating maximum–likelihood phylogenies. Mol. Biol. Evol. 32 (1), 268–274.
Nury, D., Thomassin, B.A., 1994. Paléoenvironnements tropicaux, marins et lagunaires

d'un littoral abrité (fonds meubles à bancs coralliens, lagune évaporitique) à l'Oligocène terminal (région d'Aix-Marseille). Géol. Méditerr 21, 95–108.
Pirie, M.D., Litsios, G., Bellstedt, D.U., Salamin, N., Kissling, J., 2015. Back to Gondwanaland: can ancient vicariance explain (some) Indian Ocean disjunct plant distributions? Biol. Lett. 11 (6), 20150086.
Plummer, M., Best, N., Cowles, K., Vines, K., 2006. CODA: convergence diagnosis and output analysis for MCMC. R News 6 (1), 7–11.
Prothero, D.R., Sanchez, F., 2004. Magnetic stratigraphy of the upper Eocene Florissant Formation, Teller County, Colorado. In: Lucas, S.G., Zeigler, K.E., Kondrashov, P.E. (Eds.), Paleogene Mammals. New Mexico Museum of Natural History and Science Bulletin. pp. 129–135.
Pyron, R.A., 2014. Biogeographic analysis reveals ancient continental vicariance and recent oceanic dispersal in amphibians. Syst. Biol. 63 (5), 779–797.
Rabosky, D.L., 2014. Automatic detection of key innovations, rate shifts, and diversity-dependence on phylogenetic trees. PloS One 9 (2), e89543.
Rabosky, D.L., Donnellan, S.C., Grundler, M., Lovette, I.J., 2014. Analysis and visualization of complex macroevolutionary dynamics: an example from Australian scincid lizards. Syst. Biol. 63 (4), 610–627.
Rabosky, D.L., Mitchell, J.S., Chang, J., 2017. Is BAMM flawed? Theoretical and practical concerns in the analysis of multi-rate diversification models. Syst. Biol. 66 (4), 477–498.
Ree, R.H., Smith, S.A., 2008. Maximum likelihood inference of geographic range evolution by dispersal, local extinction, and cladogenesis. Syst. Biol. 57 (1), 4–14.
Ree, R.H., Moore, B.R., Webb, C.O., Donoghue, M.J., 2005. A likelihood framework for inferring the evolution of geographic range on phylogenetic trees. Evolution 59 (11), 2299–2311.
Ritzkowski, S., 1997. K-ar-altersbestimmungen der bernsteinführenden sedimente des samlandes (paläogen, bezirk kaliningrad). Metalla (Sonderheft) 66, 19–23.
Ronquist, F., 1997. Dispersal–vicariance analysis: a new approach to the quantification of historical biogeography. Syst. Biol. 46 (1), 195–203.
Ronquist, F., Teslenko, M., Van Der Mark, P., Ayres, D.L., Darling, A., Höhna, S., Larget, B., Liu, L., Suchard, M.A., Huelsenbeck, J.P., 2012. MrBayes 3.2: efficient Bayesian phylogenetic inference and model choice across a large model space. Syst. Biol. 61 (3), 539–542.
Seton, M., Müller, R.D., Zahirovic, S., Gaina, C., Torsvik, T., Shephard, G., Talsma, A., Gurnis, M., Turner, M., Maus, S., Chandler, M., 2012. Global continental and ocean basin reconstructions since 200Ma. Earth-Sci. Rev. 113 (3), 212–270.
Shimodaira, H., 2002. An approximately unbiased test of phylogenetic tree selection. Syst. Biol. 51 (3), 492–508.
Shimodaira, H., Hasegawa, M., 1999. Multiple comparisons of log-likelihoods with applications to phylogenetic inference. Mol. Biol. Evol. 16 (8), 1114–1116.
Short, A.E.Z., Fikáček, M., 2013. Molecular phylogeny, evolution and classification of the Hydrophilidae (Coleoptera). Syst. Entomol. 38 (4), 723–752.
Short, A.E.Z., Cole, J., Toussaint, E.F.A., 2017a. Phylogeny, classification, and evolution of the water scavenger beetle tribe Hydrobiusini inferred from morphology and molecules (Coleoptera: Hydrophilidae: Hydrophilinae). Syst. Entomol. 42 (4), 677–691.
Short, A.E.Z., Post, D., Toussaint, E.F.A., 2017b. Biology, distribution, and phylogenetic placement of the California endemic water scavenger beetle *Hydrochara ricksecker*i (Horn) (Coleoptera: Hydrophilidae). Coleopt. Bull. 71 (3), 461–467.
Stadler, T., 2011. Mammalian phylogeny reveals recent diversification rate shifts. Proc. Natl. Acad. Sci. USA 108 (15), 6187–6192.
Strimmer, K., Rambaut, A., 2002. Inferring confidence sets of possibly misspecified gene trees. Proc. R. Soc. B 269 (1487), 137–142.
Thomas, N., Bruhl, J.J., Ford, A., Weston, P.H., 2014. Molecular dating of Winteraceae reveals a complex biogeographical history involving both ancient Gondwanan vicariance and long-distance dispersal. J. Biogeogr. 41 (5), 894–904.
Toussaint, E.F.A., Balke, M., 2016. Historical biogeography of Polyura butterflies in the oriental Palaeotropics: trans-archipelagic routes and South Pacific island hopping. J. Biogeogr. 43 (8), 1560–1572.
Toussaint, E.F.A., Short, A.E.Z., 2017. Biogeographic mirages? Molecular evidence for dispersal–driven evolution in Hydrobiusini water scavenger beetles. Syst. Entomol. 42 (4), 692–702.
Toussaint, E.F.A., Fikáček, M., Short, A.E.Z., 2016. India-Madagascar vicariance explains cascade beetle biogeography. Biol. J. Linn. Soc. 118, 982–991.
Toussaint, E.F.A., Bloom, D., Short, A.E.Z., 2017a. Cretaceous West Gondwana vicariance shaped giant water scavenger beetle biogeography. J. Biogeogr. 44 (9), 1952–1965.
Toussaint, E.F.A., Hendrich, L., Hájek, J., Michat, M.C., Panjaitan, R., Short, A.E.Z., Balke, M., 2017b. Evolution of Pacific Rim diving beetles sheds light on Amphi-Pacific biogeography. Ecography 40 (4), 500–510.
Toussaint, E.F.A., Seidel, M., Arriaga-Varela, E., Hajek, J., Kral, D., Sekerka, L., Short, A.E.Z., Fikáček, M., 2017c. The peril of dating beetles. Syst. Entomol. 42 (1), 1–10.
Trifinopoulos, J., Nguyen, L.T., von Haeseler, A., Minh, B.Q., 2016. W-IQ–TREE: a fast online phylogenetic tool for maximum likelihood analysis. Nucl. Acids Res. 44 (W1), W232–W235.
Turner, S., Bean, L.B., Dettmann, M., McKellar, J.L., McLoughlin, S., Thulborn, T., 2009. Australian Jurassic sedimentary and fossil successions: current work and future prospects for marine and non-marine correlation. GFF 131 (1–2), 49–70.
Von Humboldt, A., 1805. Essai sur la géographie des plantes, accompagné d'un tableau physique des régions équinoxiales. Levarault Schoell, Paris, France.
Wallace, A.R., 1876. The Geographical Distribution of Animals: With a Study of the Relations of Living and Extinct Faunas as Elucidating the Past Changes of the Earth's Surface: In Two Volumes.
Warnock, R.C., Parham, J.F., Joyce, W.G., Lyson, T.R., Donoghue, P.C., 2015. Calibration uncertainty in molecular dating analyses: there is no substitute for the prior evaluation of time priors. Proc. R. Soc. B 282 (1798), 20141013.
Wegener, A., 1912. Die entstehung der kontinente. Geologische Rundschau 3 (4), 276–292.
Xie, W., Lewis, P.O., Fan, Y., Kuo, L., Chen, M.H., 2011. Improving marginal likelihood estimation for Bayesian phylogenetic model selection. Syst. Biol. 60 (2), 150–160.
Zherikhin, V.V., Mostovski, M.B., Vršanský, P., Blagoderov, V.A., Lukashevitsh, E., 1998. The unique Lower Cretaceous locality Baissa and other contemporaneous fossil sites in North and West Transbaikalia. Proc. First Int. Paleoentomol. Conf. 185–191.